

Analytic model for a dual frequency capacitive discharge

H. C. Kim, J. K. Lee,^{a)} and J. W. Shon^{b)}

Department of Electronic and Electrical Engineering, Pohang University of Science and Technology, Pohang 790-784, South Korea

(Received 8 August 2003; accepted 19 August 2003)

A homogeneous plasma model for dual radio-frequency (rf) discharges driven by two sinusoidal current sources has been analyzed. Under the assumptions of time-independent and collisionless ion motion and inertialess electrons, the analytic expressions for discharge parameters are obtained as a function of the effective parameters such as effective frequency, effective current, and effective voltage. Effective parameters are determined by the ratio of two currents or voltages. Two rf sources are generally coupled to each other through the plasma medium. It is also shown that the reduction of the bulk plasma length due to the sheath size has to be considered for calculating the discharge parameters since the sheath length is not always negligible compared to the bulk plasma length. Furthermore, the dependence of discharge parameters on the low frequency is presented. © 2003 American Institute of Physics. [DOI: 10.1063/1.1621000]

I. INTRODUCTION

Plasma processing is an essential part for manufacturing the ultralarge scale integrated (ULSI) circuits. However, there are several issues to be solved in plasma processing using capacitively coupled radio-frequency (rf) discharges, such as the independent control of the ion flux and the ion bombardment energy, elimination of notch (local side-wall etching), increment of the plasma density, and enhancement of etching selectivity and anisotropy. As the device geometry shrinks and aspect ratio becomes higher, the restrictions become more severe. Hence, conventional capacitive reactors with a single rf (13.56 MHz) source have been continuously modified for further improvements of their performance. For example, dual frequency (DF) capacitive coupled plasmas (CCPs) operated with two distinct power sources have attracted much attention.¹⁻⁹

Goto *et al.*^{1,2} demonstrated the independent control of the ion density and the ion bombardment energy by selecting appropriate excitation frequencies in a dual rf excitation system and found that the self-bias voltage varied as a logarithmic function of the excitation frequency. Tsai *et al.*³ achieved the high selectivity plasma etching of SiO₂ with a dual frequency capacitive rf discharge. Through particle-in-cell simulations, they also found that the plasma density scales with the square of the source frequency while it remains relatively independent of the substrate frequency. Kim and Manousiouthakis⁴ presented two-dimensional simulation results for a dually excited capacitive rf plasma system using a three moment fluid model. They showed that the ion bombardment energy is a linear (logarithmic) function of the secondary rf power (frequency). Rauf and Kushner⁵ investigated the nonlinear interaction of multiple frequency sources in capacitively and inductively coupled rf excited plasma by using their plasma equipment model. Kitajima *et al.*^{6,7}

achieved the functional separation of low frequency biasing and high frequency sustaining voltages in two-frequency capacitively coupled plasma by increasing the sustaining frequency to very high frequency (100 MHz). Robiche *et al.*⁸ presented the analytic model of a dual frequency capacitive sheath. They found good quantitative agreement with particle-in-cell plasma simulations.

Capacitively coupled rf discharges have been extensively studied for the last decades because of their interesting physics as well as their widespread applications.^{10,11} The various sheath models which account for the nonlinear characteristics of the sheath dynamics have been developed.¹²⁻¹⁴ Several kinds of the discharge transitions such as the transition from stochastic to collisional electron heating,¹⁵ the transition from the low-voltage to the high-voltage mode,¹⁶ and the transition from electron-dominated to ion-dominated power dissipation¹⁷⁻¹⁹ have been observed in rf capacitive discharges. Although only two additional parameters of the frequency and power of secondary rf source are introduced in DF CCP, they give us much more complication than conventional ones in understanding the physics. The physics of DF CCP has not been fully investigated as that of CCP has been, and few analytic works^{8,9} have been offered that would give us an insight into plasma characteristics for a wide range of plasma control parameters.

In this paper, we report on the analytic solution of a homogeneous model for DF CCP as a generalization of that for CCP of Ref. 20. The analytic model is described in Sec. II. The analytic expressions are obtained for discharge parameters such as the plasma density, the plasma potential, and the powers dissipated by electrons and ions. Section III shows the dependence of several discharge parameters on the currents and low frequency by using the analytic expressions of Sec. II. Finally, our works are summarized and discussed in Sec. IV.

II. DESCRIPTION OF THE ANALYTIC MODEL

One of the earliest and simplest models for CCP is the homogeneous model of symmetrically driven rf

^{a)}Electronic mail: jkl@postech.ac.kr

^{b)}Also at LAM Research Corporation, 4650 Cushing Parkway, Fremont, CA 54538.

discharges.^{12,21} As a generalization of this model, we describe the DF capacitive sheath model for a homogeneous ion distribution. For simplicity, we assume the following plasma conditions. First, the gap distance L between electrodes at $x=0$ and $x=L$ is assumed to be small compared to the electrode diameter so that the system can be approximated as a one-dimensional plasma model. Second, the electron Debye length at the plasma-sheath boundary is negligible compared to the sheath length so that the electrons are positioned only in the plasma bulk. Third, it is assumed that the ion density is uniform everywhere and the ion motion in the sheath is collisionless. Fourth, two rf frequencies should satisfy the plasma opacity condition in the external rf field,

$$\frac{w_{pe}^2}{w^2} \gg \left(1 + \frac{\nu_m^2}{w^2}\right)^{1/2} \quad (1)$$

and

$$\frac{w_{pi}^2}{w^2} \ll 1, \quad (2)$$

where ν_m is the electron-neutral collision frequency and w_{pe} and w_{pi} are the electron and ion plasma frequencies, respectively. Consequently, the ions respond only to the time-averaged electric field while the electrons respond to the instantaneous electric field. The displacement current and the conduction current are dominant in the sheath and bulk plasma, respectively. Fifth, two frequencies should also be larger than the electron-energy relaxation frequency so that the plasma density and the electron temperature do not change much during the rf period. Thus, the density of the immobile ions is constant in time and space: $n_i(x,t) = n = \text{const}$. The electrons and hence the plasma-sheath boundary oscillate back and forth between two electrodes positioned at $x=0$ and $x=L$.

Since the discharge is symmetric, we first derive the analytic expression for the left-hand-side sheath with the electrode at $x=0$. The net charge density ρ is given by

$$\begin{aligned} \rho(x,t) &= n_i(x,t) - n_e(x,t) \\ &= n, \quad x < s(t) \\ &= 0, \quad x > s(t), \end{aligned} \quad (3)$$

where n_e is the electron density and $s(t)$ is the position of the plasma-sheath boundary. Then, the instantaneous electric field $E(x,t)$ can be obtained from Poisson's equation

$$\begin{aligned} \frac{\partial E}{\partial x} &= \frac{en}{\epsilon_0}, \quad x < s(t) \\ &= 0, \quad x > s(t), \end{aligned} \quad (4)$$

where $\epsilon_0 = 8.85 \times 10^{-12} \text{ Fm}^{-1}$ is the permittivity of free space. The integration of Eq. (4) with the boundary condition $E(x=s) \approx 0$ leads to the following solution for the electric field:

$$\begin{aligned} E(x,t) &= \frac{en}{\epsilon_0}(x-s(t)), \quad x < s(t) \\ &= 0, \quad x > s(t). \end{aligned} \quad (5)$$

The discharge is driven with the sum of two sinusoidal rf currents oscillating at two different frequencies f_l ($= w_l/2\pi$) and f_h ($= w_h/2\pi$),

$$J_{\text{rf}}(t) = J_l \cos(w_l t) + J_h \cos(w_h t), \quad (6)$$

where the subscripts l and h represent the high- and low-frequency sources, respectively. The displacement current flowing through the sheath into the plasma is defined by

$$J_d = \epsilon_0 \frac{\partial E}{\partial t}. \quad (7)$$

Substituting the electric field for $x < s(t)$, Eq. (5), Eq. (7) becomes

$$J_d = -en \frac{ds(t)}{dt}. \quad (8)$$

When the driven current is assumed to flow the sheath entirely as the displacement current, we obtain $s(t)$ by equating Eq. (6) to Eq. (8):

$$s(t) = \bar{s} - s_l \sin(w_l t) - s_h \sin(w_h t) \quad (9)$$

with

$$s_{l,h} = \frac{J_{l,h}}{enw_{l,h}}, \quad (10)$$

where \bar{s} is the time-averaged sheath length. In addition, the following relation is obtained:

$$J_{l,h} = -enu_{l,h}. \quad (11)$$

Since the minimum value of $s(t)$ should be zero, the time-averaged sheath length is given by

$$\bar{s} = s_l + s_h. \quad (12)$$

Thus, Eq. (9) becomes

$$s(t) = s_l(1 - \sin(w_l t)) + s_h(1 - \sin(w_h t)). \quad (13)$$

From Eq. (5), the voltage across the sheath with respect to the plasma potential is given by

$$V_L(t) = \int_0^{s(t)} E dx = -\frac{en}{\epsilon_0} \frac{s^2}{2}. \quad (14)$$

Inserting Eq. (9), it becomes

$$\begin{aligned} V_L(t) &= -\frac{en}{2\epsilon_0} [s_l^2(1 - \sin(w_l t))^2 + s_h^2(1 - \sin(w_h t))^2 \\ &\quad + 2s_l s_h(1 - \sin(w_l t))(1 - \sin(w_h t))]. \end{aligned} \quad (15)$$

By averaging Eq. (15) over a period, we obtain the time-averaged plasma potential:

$$\bar{V} = \frac{en}{\epsilon_0} \left[\frac{3}{4}(s_l^2 + s_h^2) + s_l s_h \right]. \quad (16)$$

For the right-hand-side sheath, the voltage across the sheath is given by

$$\begin{aligned} V_R(t) &= -\frac{en}{2\epsilon_0} [s_l^2(1 + \sin(w_l t))^2 + s_h^2(1 + \sin(w_h t))^2 \\ &\quad + 2s_l s_h(1 + \sin(w_l t))(1 + \sin(w_h t))]. \end{aligned} \quad (17)$$

From Eqs. (15) and (17), the voltage between two electrodes is obtained,

$$V(t) = V_L(t) - V_R(t) = \frac{2en\bar{s}}{\epsilon_0} [s_l \sin(w_l t) + s_h \sin(w_h t)]. \quad (18)$$

It is noted that the voltage between two electrodes can be represented as the sum of two sinusoidal functions:

$$V(t) = V_l \sin(w_l t) + V_h \sin(w_h t) \quad (19)$$

with the amplitudes of

$$V_{l,h} = \frac{2en}{\epsilon_0} \bar{s} s_{l,h}. \quad (20)$$

In addition, we obtain the following relation by using Eqs. (10) and (20):

$$f_l \frac{V_l}{J_l} = f_h \frac{V_h}{J_h}. \quad (21)$$

Substituting Eqs. (12) and (20), the time-averaged voltage of Eq. (16) can be expressed as a function of the amplitudes of two sinusoidal voltages:

$$\bar{V} = \frac{3}{8} V_{\text{eff}} \quad (22)$$

with the effective voltage

$$V_{\text{eff}} = V_l + V_h - \frac{2}{3} \frac{V_l V_h}{V_l + V_h}. \quad (23)$$

The electron power is dissipated through the ohmic heating and stochastic heating. The ohmic heating is due to the energy gain from the electric field between electron-neutral collisions. To calculate the ohmic power, we assume that the electric field in the bulk is expressed as the sum of two sinusoidal functions,

$$E(t) = E_l \sin(w_l t) + E_h \sin(w_h t). \quad (24)$$

When the driven current is assumed to flow the bulk plasma entirely as the conduction current, the power deposited by the ohmic heating per unit volume is given by

$$J(t)E(t) = J_l E_l \cos^2(w_l t) + J_h E_h \cos^2(w_h t) + [J_l E_h + J_h E_l] \cos(w_l t) \cos(w_h t). \quad (25)$$

By averaging Eq. (25) over a period, the time-averaged power per unit volume is obtained,

$$p_{e,\text{ohm}} = \frac{1}{2} (J_l E_l + J_h E_h), \quad (26)$$

which is the same as the sum of the powers contributed by two single rf sources. From the expression for the ohmic power of the single rf source,²⁰ we obtain the time-averaged power per unit area after integrating Eq. (26) over the bulk plasma,

$$\bar{S}_{e,\text{ohm}} = \frac{1}{2} R_{\text{ohm}} (J_l^2 + J_h^2) \quad (27)$$

with

$$R_{\text{ohm}} = \frac{m \nu_m d}{e^2 n}, \quad (28)$$

where m and d is the electron mass and the length of the bulk plasma, respectively. On the other hand, the stochastic heating is due to the interaction between electrons and oscillating sheaths dominantly on the plasma-sheath boundary.

For the ‘‘hard wall’’ model of the sheath, the power deposited by the stochastic heating per unit area is given by²⁰

$$S_{\text{stoc}} = -2m \int_0^\infty u_s (u - u_s)^2 f_s(u, t) du. \quad (29)$$

From Eq. (13), the oscillating sheath velocity is given by

$$u_s = \frac{ds(t)}{dt} = u_l \cos(w_l t) + u_h \cos(w_h t) \quad (30)$$

with

$$u_{l,h} = -s_{l,h} w_{l,h}. \quad (31)$$

By averaging Eq. (29) over a period along with the substitution of Eq. (30), we obtain the time-averaged stochastic heating power per unit area,

$$\bar{S}_{\text{stoc}} = \frac{1}{2} m (u_l^2 + u_h^2) n \bar{v}_e, \quad (32)$$

where \bar{v}_e is the mean electron speed ($= \sqrt{8eT_e/\pi m}$, where T_e is the electron temperature in unit of volts). With the substitution of Eq. (11), Eq. (32) becomes

$$\bar{S}_{\text{stoc}} = \frac{1}{2} R_{\text{stoc}} (J_l^2 + J_h^2) \quad (33)$$

with

$$R_{\text{stoc}} = \frac{m \bar{v}_e}{e^2 n}. \quad (34)$$

By adding the stochastic heating for two sheaths and the ohmic heating from Eqs. (27) and (33), the total time-averaged electron power per unit area becomes

$$S_e = \bar{S}_{\text{ohm}} + \bar{S}_{\text{stoc}} = \frac{1}{2} R_{\text{eff}} J_{\text{eff}}^2 \quad (35)$$

with $R_{\text{eff}} = R_{\text{ohm}} + 2R_{\text{stoc}}$ and the effective current

$$J_{\text{eff}} = \sqrt{2} J_{\text{rms}}, \quad (36)$$

where $J_{\text{rms}} = \sqrt{(J_l^2 + J_h^2)/2}$ is the root-mean-square (rms) value of the applied rf current J_{rf} .

By equating Eq. (35) to the electron energy lost,

$$S_e = 2en u_B (\epsilon_c + \epsilon_e), \quad (37)$$

the plasma density is obtained

$$n = \frac{1}{2} \left[\frac{m (\nu_m d + 2\bar{v}_e)}{e^3 u_B (\epsilon_c + \epsilon_e)} \right]^{1/2} J_{\text{eff}}, \quad (38)$$

where ϵ_c and ϵ_e are collisional loss per electron-ion pair created and mean kinetic energy lost per electron ($= 2T_e$), respectively. u_B is the Bohm velocity ($= \sqrt{eT_e/M}$, where M is the ion mass).

The time-averaged power dissipated by ion acceleration is given by²⁰

$$S_i = 2en u_B \left(\bar{V} + \frac{T_e}{2} \right). \quad (39)$$

From Eqs. (10) and (16), Eq. (39) can be expressed as the function of the currents and frequencies,

$$S_i = \frac{3u_B}{2\epsilon_0} \left(\frac{J_l^2}{w_l^2} + \frac{J_h^2}{w_h^2} + \frac{4}{3} \frac{J_l J_h}{w_l w_h} \right) + en u_B T_e. \quad (40)$$

It can also be represented as a function of the effective frequency $f_{\text{eff}} (= w_{\text{eff}}/2\pi)$ and the effective current J_{eff} :

$$S_i = \frac{3u_B}{2\epsilon_0} \left(\frac{J_{\text{eff}}}{w_{\text{eff}}} \right)^2 + enu_B T_e \quad (41)$$

with

$$w_{\text{eff}}^2 = \frac{w_h^2(w_l J_h)^2 + w_l^2(w_h J_l)^2}{(w_l J_h)^2 + 4(w_l J_h)(w_h J_l)/3 + (w_h J_l)^2}. \quad (42)$$

From Eqs. (22), (35), (38), and (41), it is noted that the discharge parameters of DF CCP, such as the plasma density, the plasma potential, and the powers dissipated by electrons and ions, can be expressed just as those of CCP driven with effective parameters, such as the effective current, effective voltage, and effective frequency. Since the effective frequency in DF CCP is dependent on the currents in contrast to the frequency in CCP, DF CCP can be considered as CCP with a variable (effective) frequency.⁹ With this concept, it has been explained that the ion flux and the ion bombardment energy in DF CCP can be controlled by the high-frequency current and the low-frequency current, respectively, under certain plasma parameter regimes. It is also found that effective parameters in Eqs. (43)–(45) are not represented as the linear sum of two driving parameters. In other words, two current sources are generally coupled to each other. A similar nonlinear interaction of multiple frequency sources through the nonlinear plasma medium has also been found by Rauf *et al.*⁵ in a hybrid simulation.

The effective parameters have to be determined by the competition of two rf sources. When we use terms “primary” for a rf source with the fixed current and “secondary” for the other, the effective parameters of Eqs. (23), (36), and (42) can be expressed as a function of the ratio of two currents or voltages:

$$V_{\text{eff}}(V_p, V_r) = V_p \left(1 + V_r - \frac{2}{3} \frac{V_r}{1 + V_r} \right), \quad (43)$$

$$J_{\text{eff}}(J_p, J_r) = J_p \sqrt{1 + J_r^2}, \quad (44)$$

and

$$f_{\text{eff}}^2(f_p, f_r, J_r) = f_p^2 \frac{1 + J_r^2}{1 + 4J_r/3f_r + J_r^2/f_r^2}, \quad (45)$$

with $V_r = V_s/V_p$, $J_r = J_s/J_p$, and $f_r = f_s/f_p$. Without the secondary current, the effective frequency of Eq. (45) is the primary frequency. As the secondary current goes to the infinity, the effective frequency becomes the secondary frequency. In particular, when the current ratio is the same as the frequency ratio, the effective frequency is

$$f_{\text{eff}}(J_r = f_r) = \sqrt{\frac{3}{5}} f_{\text{rms}}, \quad (46)$$

where $f_{\text{rms}} = \sqrt{(f_p^2 + f_s^2)/2}$ is the rms value of two frequencies.

Figure 1 shows the transition of the effective frequency from a primary frequency f_p to a secondary frequency f_s obtained from Eq. (45). As the 27 MHz current increases for the fixed 2 MHz current ($f_p = 2$ MHz, $J_p = 0.22$ mA cm⁻², and $f_s = 27$ MHz), the effective frequency increases rapidly

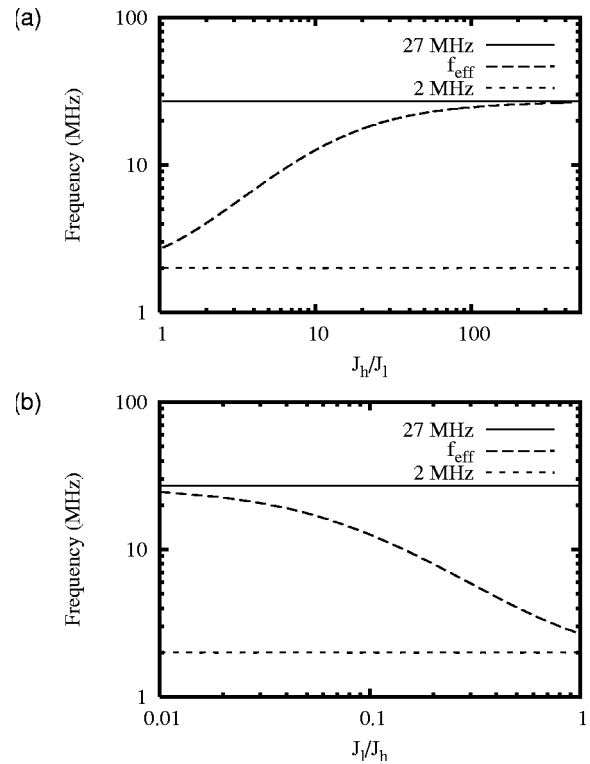


FIG. 1. Effective frequency transitions (a) when the high-frequency (27 MHz) current increases for the fixed low-frequency (2 MHz) current ($J_l = 0.22$ mA cm⁻²) and (b) when the low-frequency (2 MHz) current varies for the fixed high-frequency (27 MHz) current ($J_h = 1$ mA cm⁻²).

starting from 2 MHz and is saturated to 27 MHz, as shown in Fig. 1(a). As the 2 MHz current increases for the fixed 27 MHz current ($f_p = 27$ MHz, $J_p = 1$ mA cm⁻², and $f_s = 2$ MHz), the effective frequency changes from 27 MHz to 2 MHz, as shown in Fig. 1(b).

The bulk plasma length is given by the difference between the gap distance and the sheath length: $d = L - \bar{s}$. The sheath length and hence the bulk plasma length changes with the current and is inversely proportional to the frequency. In the CCP with the typical frequency of 13.56 MHz, the bulk plasma length is approximated to the gap distance since the sheath length is usually negligible compared to the bulk length. However, for the DF CCP, where the low frequency is typically lower than the typical frequency, it may not be satisfied any more. The details will be shown below.

III. THE RESULTS OF THE ANALYTIC MODEL

To investigate the reduction of the bulk plasma length due to the sheath size, we have obtained the bulk length as a function of the high-frequency (27 MHz) current for the fixed high-frequency current ($J_h = 1$ mA cm⁻²) or the low-frequency (2 MHz) current for the fixed low-frequency current ($J_l = 0.22$ mA cm⁻²). It was obtained for argon discharges at pressure of 100 mTorr by using Eqs. (10), (12), and (38). T_e , ϵ_c , and L were set to be 3.0 eV, 50 V, and 2.5 cm, respectively. As shown in Fig. 2(a), the bulk length is shortened significantly from the gap distance for the large low-frequency current or the small high-frequency current. For larger low-frequency current or smaller high-frequency

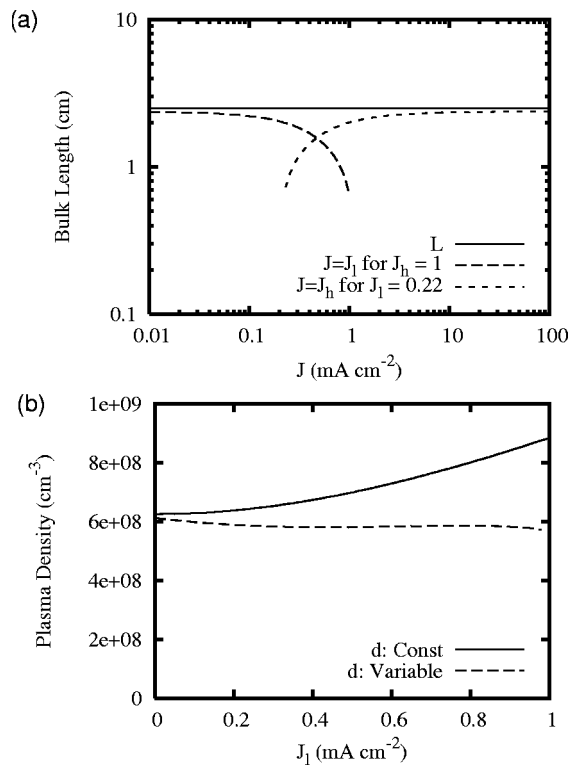


FIG. 2. (a) The bulk plasma length as a function of the high-frequency (27 MHz) current or the low-frequency (2 MHz) current. (b) The plasma density as a function of the low-frequency (2 MHz) current ($J_h = 1 \text{ mA cm}^{-2}$).

current, the plasma is not sustained any more. The effect of the reduction of the bulk length on the plasma density is also shown in Fig. 2(b). For the case where the bulk length is fixed to the gap distance ($d=L$), the plasma density increases with the low-frequency (2 MHz) current for the fixed high-frequency (27 MHz) current ($J_h = 1 \text{ mA cm}^{-2}$). However, for the self-consistent case where the bulk length is reduced by the sheath length, the plasma density does not change much with the low-frequency current. Thus, the reduction of the bulk plasma length due to the sheath size has to be considered for calculating discharge parameters in the analytic modeling of DF CCP unlike to that of typical CCP. This result is also consistent with the particle-in-cell simulation result of Babaeva *et al.*²⁵ that the increase of low-frequency voltage leads to subsequent increase in sheath width.

A power dissipation mode transition between electrons and ions originates from the different dependence of rf powers consumed by ions in sheath and electrons in the plasma body on the current. The mode transition from electron-dominated dissipation to ion-dominated dissipation has been achieved by varying plasma control parameters, such as the increase of current or the decrease of pressure, frequency, and magnetic field.¹⁷⁻¹⁹ These phenomena are observed in DF CCP by varying one of the two driving currents. Using Eqs. (35) and (41), we have obtained powers absorbed by electrons, ions, and all species, as shown in Fig. 3. The condition is the same as that in Fig. 2. As shown in Fig. 3(a), the transition occurs twice as the high-frequency current changes for the fixed low-frequency current unlike CCP because of

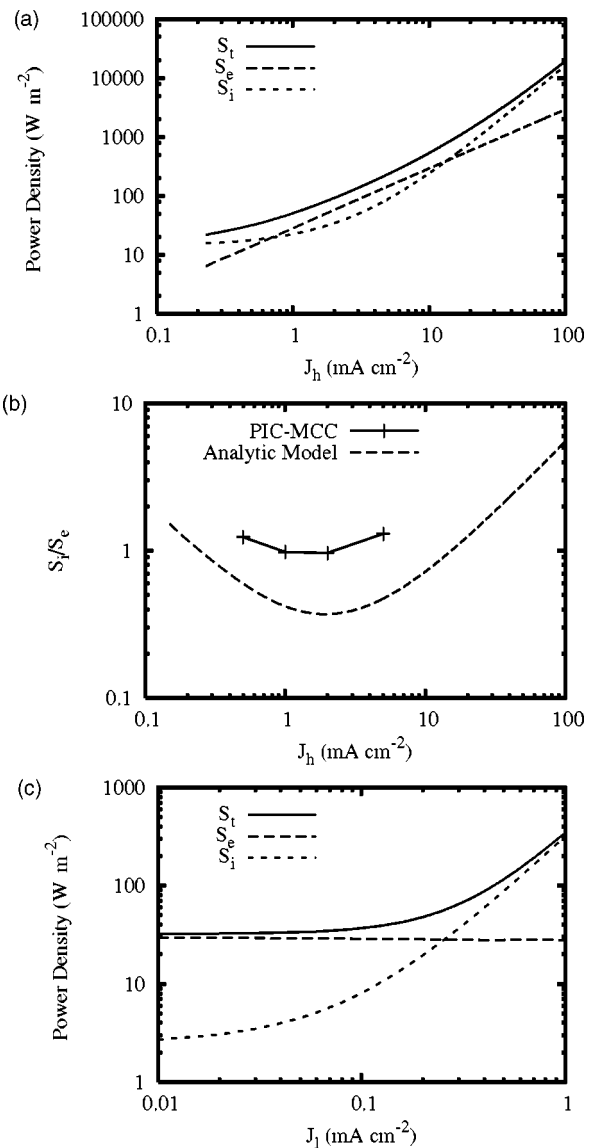


FIG. 3. Powers absorbed by electrons ions, and all species as a function of (a) the high-frequency (27 MHz) current ($J_l=0.22 \text{ mA cm}^{-2}$) and (c) the low-frequency (2 MHz) current ($J_h = 1 \text{ mA cm}^{-2}$). (b) The ratio of the ion to electron power as a function of the high-frequency (27 MHz) current ($J_l=0.14 \text{ mA cm}^{-2}$).

the effective frequency transition.⁹ Figure 3(b) shows the ratio of the ion to electron power as a function of the high-frequency current for the fixed low-frequency current ($J_l = 0.14 \text{ mA cm}^{-2}$). Our analytical result was compared with a one-dimensional electrostatic particle-in-cell (PIC) simulation with a Monte Carlo collision (MCC)^{22,23} which is a self-consistent and fully kinetic method. Two of them are qualitatively in agreement. Figure 3(c) shows that the transition from the electron-dominated mode to the ion-dominated mode as the low-frequency current increases as it does in CCP. The electron power does not change much with the low-frequency current like the plasma density in Fig. 1(b).

The current-voltage relation is one of the basic electrical characteristics in CCP.²⁴ Figure 4 shows the time-averaged plasma potential and the amplitudes of the low-frequency and high-frequency voltages as a function of the high-

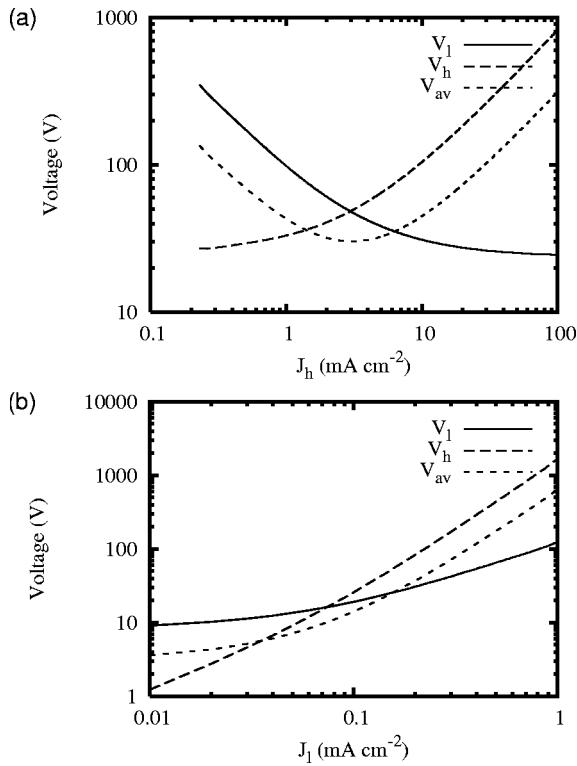


FIG. 4. The time-averaged plasma potential and the amplitudes of the low-frequency (2 MHz) and high-frequency (27 MHz) voltages as a function of (a) the high-frequency (27 MHz) current ($J_h=0.22$ mA cm⁻²) and (b) low-frequency (2 MHz) current ($J_l=1$ mA cm⁻²). V_{av} is the time-averaged plasma potential.

frequency or low-frequency current. They were obtained from Eqs. (20), (10), (22), and (23). Since two rf sources are coupled to each other, both of the high-frequency and low-frequency voltages change with one of two currents even though the current of the other source is fixed. Both of the high-frequency and low-frequency voltages increase with the low-frequency current in entire regime, as shown in Fig. 4(b). However, as shown in Fig. 4(a), the low-frequency voltage and hence the plasma potential decrease with the high-frequency current in the regime of a small high-frequency current. We can derive the mathematical expression of $\text{sgn}[dV_p/dJ_s]$ which determines whether one of two voltages increases with the current of the other source or not. From Eq. (21), it becomes

$$\text{sgn}\left[\frac{dV_p}{dJ_s}\right] = \text{sgn}\left[\frac{d(V_s/J_s)}{dJ_s}\right]. \quad (47)$$

When the voltage is expressed as a function of the plasma density, currents, and frequencies from Eqs. (10) and (20), Eq. (47) becomes

$$\text{sgn}\left[\frac{dV_p}{dJ_s}\right] = \text{sgn}\left[\frac{1}{nf_s} - \frac{1}{n^2}\left(\frac{J_s}{f_s} + \frac{J_p}{f_p}\right)\frac{dn}{dJ_s}\right]. \quad (48)$$

By using Eq. (38), Eq. (48) is reduced to

$$\text{sgn}\left[\frac{dV_p}{dJ_s}\right] = \text{sgn}[f_p J_p - f_s J_s]. \quad (49)$$

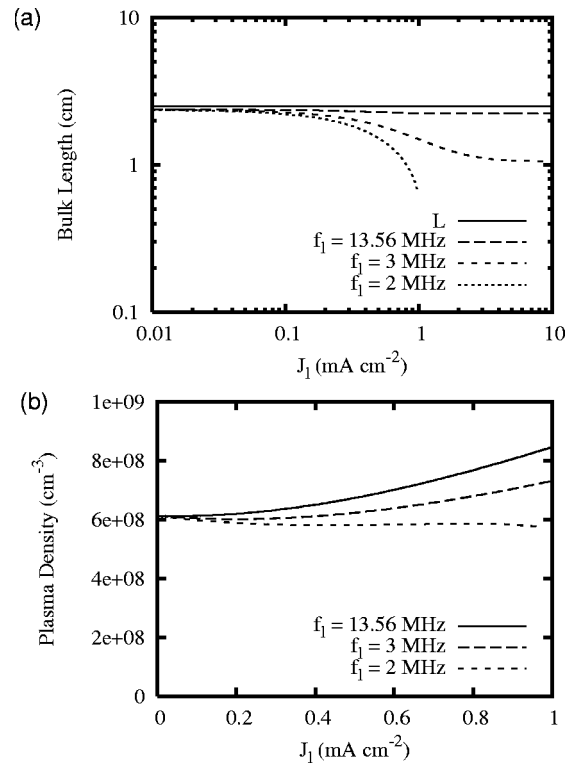


FIG. 5. For various low frequencies, (a) the bulk plasma length and (b) the plasma density as a function of the low-frequency current ($L=2.5$ cm and $J_h=1$ mA cm⁻²).

Therefore, when $f_p J_p < f_s J_s$ is satisfied, the primary voltage V_p decreases with the secondary current J_s . Otherwise, the primary voltage V_p increases with the secondary current J_s .

Since the sheath length is affected mainly by the low-frequency source, we have investigated the effect of the low frequency on the bulk length and the plasma density for various low frequencies ($L=2.5$ cm), as shown in Fig. 5. For the large low frequency, the bulk length is not much shortened with the low-frequency current [Fig. 5(a)] and hence the plasma density increases with the low frequency current [Fig. 5(b)]. Figure 6 shows the results for the longer gap distance of $L=5$ cm. Compared to the case of the short gap distance, the bulk length changes weakly with the low-frequency current [Fig. 6(a)]. Hence, even for 2 MHz, the plasma density increases with the low-frequency current [Fig. 6(b)]. It is also noted that the dependence of the plasma density on the low frequency is different for the different gap distances. For the short gap distance ($L=2.5$ cm), we can find the regime where the plasma density increases significantly with the low frequency for the same low-frequency current [Fig. 5(b)]. However, for the long gap distance ($L=5$ cm), the plasma density does not change much with the low frequency [Fig. 6(b)].

For the high frequency of 27 MHz and the low frequency of 2 MHz, it has been found that a power dissipation mode transition occurs twice as the high-frequency current and hence the effective current change.⁹ It was due to the significant change of the the effective frequency. Figure 7 shows the dissipated powers as a function of the effective current for the low frequency of 13.56 MHz when the high-

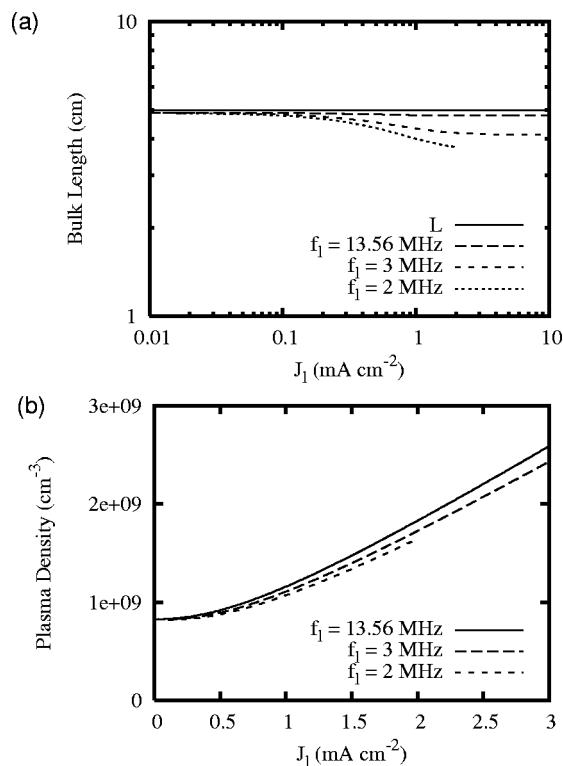


FIG. 6. For the gap distance of 5 cm, (a) the bulk plasma length and (b) the plasma density as a function of the low-frequency current ($J_1 = 1 \text{ mA cm}^{-2}$).

frequency (27 MHz) current varies for the fixed low-frequency current. Unlike the case of the low frequency of 2 MHz, the mode transition happens once just as CCP. It is because the high frequency and the low frequency are close to each other and hence the change of the effective frequency is not so significant.

IV. CONCLUSIONS

We have analyzed a homogeneous plasma model for dual rf discharges driven by two sinusoidal current sources. Under the assumptions of time-independent and collisionless ion motion and inertialess electrons, the analytic expressions

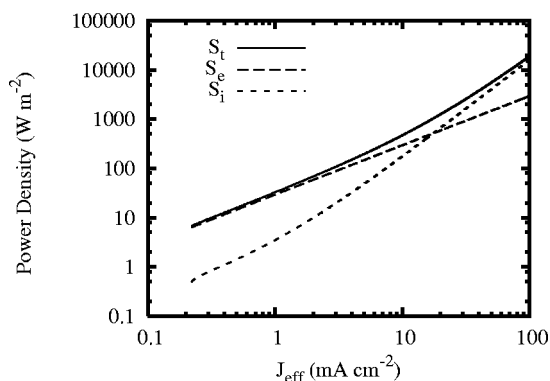


FIG. 7. The dissipated powers as a function of the effective current for the low frequency of 13.56 MHz when the high-frequency (27 MHz) current varies for the fixed low-frequency current ($J_1 = 0.22 \text{ mA cm}^{-2}$).

are obtained for the rf discharge parameters such as the plasma density, the plasma potential, and the powers dissipated by electrons and ions. They can be expressed as a function of the effective parameters such as effective frequency, effective current, and the effective voltage. Effective parameters are determined by the ratio of two currents or voltages as a consequence of the competition of two rf sources. Two rf sources are generally coupled to each other through the nonlinear plasma medium. It is also shown that the reduction of the bulk plasma length due to the sheath size has to be considered for calculating discharge parameters in the analytic modeling of DF CCP since the sheath length is not always negligible compared to the bulk plasma length. The reduction of the bulk length is significant for the short gap distance. Furthermore, the dependence of discharge parameters on the low frequency was also presented.

ACKNOWLEDGMENTS

Discussions with Dr. N. Yu. Babaeva and Dr. O. V. Manuilenko are greatly acknowledged.

This work was supported in part by the LAM Research Corporation, Samsung Electronics, and Korea Research Foundation Grant (KRF-2000-015-DS0010).

- ¹H. H. Goto, H.-D. Lowe, and T. Ohmi, *J. Vac. Sci. Technol. A* **10**, 3048 (1992).
- ²H. H. Goto, H.-D. Lowe, and T. Ohmi, *IEEE Trans. Semicond. Manuf.* **6**, 58 (1993).
- ³W. Tsai, G. Mueller, R. Lindquist, and B. Frazier, *J. Vac. Sci. Technol. B* **14**, 3276 (1996).
- ⁴H. C. Kim and V. I. Manousiouthakis, *J. Vac. Sci. Technol. A* **16**, 2162 (1998).
- ⁵S. Rauf and M. J. Kushner, *IEEE Trans. Plasma Sci.* **27**, 1329 (1999).
- ⁶T. Kitajima, Y. Takeo, and T. Makabe, *J. Vac. Sci. Technol. A* **17**, 2510 (1999).
- ⁷T. Kitajima, Y. Takeo, Z. L. Petrovic, and T. Makabe, *Appl. Phys. Lett.* **77**, 489 (2000).
- ⁸J. Robiche, P. C. Boyle, M. M. Turner, and A. R. Ellingboe, *J. Phys. D* **36**, 1810 (2003).
- ⁹H. C. Kim, J. K. Lee, and J. W. Shon, "Dual radio-frequency discharges: effective frequency concept," *Appl. Phys. Lett.* (submitted).
- ¹⁰V. A. Godyak, *Soviet Radio Frequency Discharge Research* (Delphic Associates, Inc., Falls Church, VA, 1986).
- ¹¹M. A. Lieberman and A. J. Lichtenberg, *Principles of Plasma Discharges and Materials Processings* (Wiley, New York, 1994).
- ¹²V. A. Godyak, *Sov. J. Plasma Phys.* **2**, 78 (1976).
- ¹³M. A. Lieberman, *IEEE Trans. Plasma Sci.* **16**, 638 (1988).
- ¹⁴V. A. Godyak and N. Sternberg, *Phys. Rev. A* **42**, 2299 (1990).
- ¹⁵V. A. Godyak and R. B. Piejak, *Phys. Rev. Lett.* **65**, 996 (1990).
- ¹⁶V. A. Godyak, R. B. Piejak, and B. M. Alexandrovich, *Phys. Rev. Lett.* **68**, 40 (1992).
- ¹⁷V. A. Godyak, R. B. Piejak, and B. M. Alexandrovich, *J. Appl. Phys.* **69**, 3455 (1991).
- ¹⁸S. J. You, H. C. Kim, C. W. Chung, H. Y. Chang, and J. K. Lee, "The mode transition for power dissipation induced by driving frequency in capacitively coupled plasma," *J. Appl. Phys.* (to be published).
- ¹⁹S. J. You, C. W. Chung, K. H. Bai, and H. Y. Chang, *Appl. Phys. Lett.* **81**, 2529 (2002).
- ²⁰M. A. Lieberman and A. J. Lichtenberg, *Ref. 11*, pp. 328–338.
- ²¹V. A. Godyak and O. A. Popov, *Sov. J. Plasma Phys.* **5**, 227 (1979).
- ²²C. K. Birdsall, *IEEE Trans. Plasma Sci.* **19**, 65 (1991).
- ²³V. Vahedi and M. Surendra, *Comput. Phys. Commun.* **87**, 179 (1995).
- ²⁴V. A. Godyak, R. B. Piejak, and B. M. Alexandrovich, *IEEE Trans. Plasma Sci.* **19**, 660 (1991).
- ²⁵N. Babaeva, J. K. Lee, H. C. Kim, O. Manuilenko, and J. W. Shon, "Simulation of capacitively coupled single- and dual-frequency RF discharges," *IEEE Trans. Plasma. Sci.* (submitted).